Evidence that the autoimmune phenotype in mice with dendritic cell-specific deletion of Tnfaip3/ A20 is independent of the IL-23/ IL-17 axis.

Tridib Das, Ingrid Bergen, Menno van Nimwegen, Jennifer van Hulst, Geert van Loo, Bart N. Lambrecht, Mirjam Kool, Rudi W. Hendriks

Manuscript in preparation

ABSTRACT

Background: Dendritic cells (DCs) are sentinel cells within the immune system that direct tolerogenic and immune conditions. Mice that lack *Tnfaip3*/A20, a negative regulator of NF-κB signaling, specifically in DCs (*Tnfaip3*$^{CD11c\text{-}KO}$ mice) have a lupus-like autoimmune phenotype characterized by autoantibodies and glomerulonephritis. *Tnfaip3*/A20-deficient DCs display spontaneous activation and thereby induce T and B cell activation. *In vitro* co-cultures of stimulated bone marrow-derived *Tnfaip3*$^{CD11c\text{-}KO}$ DCs with T cells display increased IL-17 production.

Objective: We investigated the role of IL-23, a key cytokine for T helper 17 (Th17) cell maintenance and expansion, in the pathology of the lupus-like autoimmune phenotype of *Tnfaip3* $^{CD11c\text{-}KO}$ mice.

Methods: *Tnfaip3*$^{CD11c\text{-}KO}$ mice were crossed to *Il23*^{KO} mice and *in vivo* Th subsets, B cell activation, levels of (auto-)antibodies and kidney inflammation were assessed in 24-week-old mice.

Results: Spleens of *Tnfaip3*$^{CD11c\text{-}KO}$ mice were enlarged, but additional loss of IL-23 resulted in a substantial reduction of spleen size, granulocytes and monocytes/macrophage counts. Although DCs from *Il23*^{KO}*Tnfaip3*$^{CD11c\text{-}KO}$ had a more activated phenotype than DCs from *Il23*^{WT}*Tnfaip3*$^{CD11c\text{-}KO}$ mice, their numbers in the spleen remained very low. *In vivo* Th17 cell differentiation was not enhanced in *Tnfaip3*$^{CD11c\text{-}KO}$ mice, compared to wild-type controls littermates. Loss of IL-23 did not significantly affect the numbers of Th17 cells in the spleen. Although splenic plasma cells were essentially not altered in *Tnfaip3*$^{CD11c\text{-}KO}$ mice, they were reduced by additional IL-23-deficiency. Total IgG1 or autoreactive IgG1 was increased in the serum of both *Il23*^{KO} and *Il23*^{WT} *Tnfaip3*$^{CD11c\text{-}KO}$ mice. Only IgA was greatly reduced in *Il23*^{KO}*Tnfaip3*$^{CD11c\text{-}KO}$ mice compared to *Il23*^{WT}*Tnfaip3*$^{CD11c\text{-}KO}$ mice. Finally, IL-23-deficiency did not affect glomerulonephritis in *Tnfaip3*$^{CD11\text{-}KO}$ mice.

Conclusion: These findings indicate that the lupus-like autoimmune pathology in *Tnfaip3*$^{CD11c\text{-}KO}$ mice is independent of the IL-23/IL-17 axis.

INTRODUCTION

Systemic lupus erythematosus (SLE) is the prototypical systemic autoimmune disorder in which multiple innate and adaptive immune cells, such as dendritic cells (DCs), T cells and B cells play an important role[1]. B lymphocytes are the primary effector cells in SLE pathogenesis[2]. As they become plasma cells, they produce autoreactive antibodies and thereby facilitate immune complexes that trigger kidney inflammation[3]. In addition, an imbalanced T-helper (Th) cell differentiation has been implicated in lupus pathology, because an increase of Th17 cells or their primary cytokine IL-17 was observed in patients compared to healthy controls and correlated with more disease activity[4, 5]. Further downstream, Th17 cells are known to facilitate differentiation of B cells into plasma cells and antibody production by secretion of cytokines[6, 7]. It has been demonstrated in mice that IL-17 is indispensable for the production of several autoantibodies and for the development of lupus nephritis[8].

Differentiation and stabilization of Th17 cells is dependent on IL-23[9], which is primarily produced by activated antigen presenting cells including DCs or monocytes/macrophages[10]. IL-23R signaling is responsible for increasing RORγt expression and IL-17 via STAT3[11]. Next to its function in survival and expansion of Th17 cells[12], IL-23 is also involved in unlocking the full pathogenic potential of Th17 cells[13]. The observation that the addition of ustekinumab, a monoclonal antibody that inhibits IL-23 and IL-12, to standard-of-care treatment resulted in a better efficacy in clinical and laboratory parameters than placebo, supports further development of ustekinumab as a novel therapeutic strategy in SLE[14, 15].

Ablation of the *Tnfaip3* gene encoding A20, a negative regulator of the NF-κB signaling pathway, specifically in DCs *in vivo* (in *Tnfaip3*$^{CD11c\text{-}KO}$ mice), resulted in T cell and B cell activation, antibody class switching, systemic inflammation, and glomerulonephritis, generating a phenotype resembling SLE[16]. Stimulated DCs lacking A20/Tnfaip3 produced high levels of IL-23 and promoted IL-17 production in *in vitro* co-cultures with T cells[16]. Moreover, we recently demonstrated that A20/Tnfaip3-deficient DCs induced Th17 cell differentiation via production of the pro-inflammatory cytokines IL-1β, IL-6 and IL-23 *in vivo* in a model of allergic airway inflammation[17].

In this report, we investigated whether ablation of IL-23 would alter Th17 cell induction in *Tnfaip3*$^{CD11c\text{-}KO}$ mice *in vivo*. Th17 cells promote B cell proliferation and trigger antibody production and immunoglobulin (Ig) heavy chain class switch recombination *in vivo*[7]. Therefore, we wondered whether IL-23 abrogation would affect plasma cell differentiation and Ig production and consequently renal pathology. We found that absence of IL-23 in *Tnfaip3*$^{CD11c\text{-}KO}$ mice reduced the splenic myeloid cell populations, while increasing DC activation markers. Surprisingly, Th17 cells were not increased in 24-week-old *Tnfaip3*$^{CD11c\text{-}KO}$ mice, compared to *Tnfaip3*$^{CD11c\text{-}WT}$ mice. Moreover, the absence of IL-23 in

Tnfaip3$^{CD11c\text{-}KO}$ mice did not alter the numbers of Th17 cells or plasma cells in the spleen. Serum levels of total IgG1 and autoreactive IgG1 and kidney inflammation were also not dependent on IL-23.

MATERIALS AND METHODS

Mice

Cd11c-cre^{+} transgenic *Tnfaip3*$^{fl/fl}$ mice[16] were crossed with *Il23p19*$^{-/-}$ on a C57BL/6 background[18] to obtain *Il23*^{WT} *and Il23*^{KO} *Tnfaip3*$^{CD11c\text{-}KO}$ mice. Male and female mice were analyzed at 24-weeks of age and cre-deficient littermates were used as wild-type (WT) controls. Mice were bred and housed under specific pathogen-free conditions in the Erasmus MC experimental animal facility. All experiments were approved by the animal ethical committee of the Erasmus MC (EMC3329).

Tissue preparation

Spleens and bone marrow (BM) were taken from sacrificed mice to obtain single cell suspensions. One femur per mouse was crushed using a pestle and mortar and spleens were homogenized through a 100 µm cell strainer (Corning Inc., Corning, NY, USA) and collected in Gibco™ RPMI Medium 1640 (1 x) + GlutaMAX™-1 (Thermo Fisher Scientific Inc., Waltham, MA, USA). Red blood cells were lysed using osmotic lysis buffer (0.15 M NH_4CL, 10 mM $KHCO_3$, 0.1 mM EDTA, pH 7.1 - 7.4; sterile-filtered with 0.22 µm filter). Viable cells were counted using Tryptan blue and a Buerker-Tuerk counting chamber (Paul Marienfeld GmbH & Co. KG, Lauda Königshofen, Germany). Freshly isolated kidneys were incubated on Roti-Histofix 4% (Carl-Roth, Karlsruhe, Germany) for 24 hrs and then embedded in paraffin wax.

Periodic Acid Schiff Diastase (PAS-D) staining

Three µm-thick paraffin-embedded kidney sections were stained according to the PAS-D Staining protocol. Briefly, paraffin-embedded sections were dewaxed and hydrated to water using Xylene (Sigma-Aldrich) and ethanol dilutions in MilliQ. One part human saliva (containing the enzyme diastase) was diluted 1:10 with MilliQ and incubated on slides at room temperature for 30 min. Slides were placed in freshly prepared periodic acid solution for 5 min (Sigma-Aldrich) and subsequently in Schiff's reagent for 5 min and counterstained with Gill's hematoxylin (Merck Millipore) for 2 seconds. Finally, slides were dehydrated using Xylene and mounted in Entallan (Merck Millipore).

Immunohistochemistry of Cryosections

For immunohistochemistry, 6 µm acetone or 4 % formalin-fixed spleen sections were blocked in peroxidase blocking buffer (PBS, 0.67 % H_2O_2, 2 % NaN_3) at room temperature for 30 min. Blocking Buffer (1% Blocking Reagent (Roche Diagnostics GmbH, Mannheim, Germany) in PBS) containing 10% normal goat or donkey serum was used to prevent aspecific secondary antibody binding. Sections were stained with primary antibodies at room temperature for 1 hr, washed with PBS and incubated with alkaline phosphatase (AP) or peroxidase (PO) conjugated secondary antibodies at room temperature for 30 min. Used antibodies were: anti-GL7 (clone RUO, 1:50, eBioscience) and anti-IgD-PE (clone 11-26, 1:50, eBioscience) with alkaline phosphatase (AP)-conjugated goat anti-rat (1:50, Jackson Immunoresearch) and peroxidase-labeled goat anti-PE, 1:50, Rockland Immunochemichals) as secondary antibody, respectively. AP was detected first during 30 min using a mixture containing N-(4-Amino-2,5-diethoxyphenyl)benzamide (Fast Blue BB, Sigma-Aldrich), 2 M HCl, 4 % $NaNO_2$, Naphthol AS-MX phosphate (VWR International, Radnor, PA, USA), N,N-dimethylformamide (DMF) (Sigma-Aldrich), Tris-HCl buffer (pH 8.5) and (-)-tetramisole hydrochloride (Sigma-Aldrich). The substrate was filtered using filtration paper. Secondly, peroxidase was detected within 30 min with a mixture containing 3-amino-9-ethylcarbazole (AEC) in DMF, 0.1 M NaAC (pH 4.6), 30% H_2O_2 (Merck Millipore, Darmstadt and double-filtered. Kaiser's Glycerol/Gelatin (Boom B.V., Meppel, The Netherlands) was used to embed tissue sections and micrographs were made using a Leica DM2000 microscope (Leica Microsystems GmbH, Wetzlar, Germany), a Leica DFC450 camera (Leica Microsystems GmbH, Wetzlar, Germany) and Leica Application (LAS) Software Version 4.5.0 (Leica Microsystems GmbH, Wetzlar, Germany).

Confocal Microscopy

For confocal imaging, 12 µm-thick spleen cryostat sections were stained as explained above. Primary and secondary antibodies were (Target, clone, dilution, manufacturer, with respective secondary antibody target, dilution, manufacturer): B220 (RA3-6B2, 1:50, BD Biosciences, Donkey anti-Rat Cy5, 1:200, Jackson Immunoresearch), CD11c (N418, 1:10, eBioscience, Goat anti-Hamster Cy3, 1:1000, Jackson Immunoresearch), CD3e (KT3, 1:50, Bioceros, Donkey anti-Rat Cy3, 1:1000, Jackson Immunoresearch). Slides were counterstained with 4′,6-diamidino-2-phenylindole (DAPI), mounted with VECTASHIELD® HardSet™ Antifade Mounting Medium (Vector Laboratries, Burlingame, CA, USA) and analyzed on a Zeiss LSM 510 META confocal microscope (Carl Zeiss AG, Oberkochen, Germany). Images were analyzed using ImageJ software (Rasband, W.S., ImageJ, U. S. National Institutes of Health, Bethesda, Maryland, USA).

Flow cytometry

Flow cytometry surface and intracellular staining procedures have been described previously[19]. Monoclonal antibodies used for flow cytometric analyses are listed in **Supplementary Table S1A.**

Immunoglobulin levels

For quantification of total immunoglobulin levels, Nunc Microwell plates (Life technologies, Carlsbad, CA, USA) were coated with 1 µg/ml goat-anti-mouse IgM, IgA, IgG1, IgG2b, IgG2c, or IgG3 (Southern Biotech, Birmingham, AL, USA) overnight at 4C°. Wells were blocked with 10% FCS (Capricorn Scientific, Ebsdorfergrund, Germany) in PBS (Thermo Scientific, Waltham, MA, USA) for 1 hr. Standards and serum were diluted in PBS and incubated at room temperature for 3 hrs. Depending on the isotype of interest, biotin labeled anti-mouse IgM, IgA, IgG1, IgG2b, IgG2c, or IgG3 (Southern Biotech) was incubated for 1 hr. Streptavidin-horseradish peroxidase (eBioscience) and 3,3',5,5'-tetramethylbenzidine substrate (eBioscience) was used to develop the ELISA and then optical density was measured at 450 nm on a Microplate Reader (Bio-Rad, Hercules, CA, USA). Ig autoreactivity assessment was assessed as previously described[20].

Statistics

If the Kruskal-Wallis 1-way ANOVA test was significant, we further used the non-parametric Mann Whitney U test to determine significant differences between two groups. P-values <0.05 were considered significant. All analyses were performed using Prism (GraphPad Software version 9, La Jolla, CA, USA). All data are presented as mean values with the standard error of the mean (SEM).

RESULTS

Lack of IL-23 strongly reduces the numbers of neutrophils, monocytes/ macrophage and DCs in *Tnfaip3*$^{CD11c\text{-}KO}$ mice.

To assess the effect of IL-23 abrogation on the phenotype of *Tnfaip3*$^{CD11c\text{-}KO}$ mice, we analyzed spleens of *Tnfaip3*$^{CD11c\text{-}WT}$, *Tnfaip3*$^{CD11c\text{-}HZ}$ and *Tnfaip3*$^{CD11c\text{-}KO}$ mice that were either WT or KO for the *IL-23* gene, at the age of 24 weeks. Spleens of the aged *Tnfaip3*$^{CD11c\text{-}KO}$ mice were enlarged, compared to *Tnfaip3*$^{CD11c\text{-}WT}$ and *Tnfaip3*$^{CD11c\text{-}HZ}$ mice (**Figure 1A**), as previously described[16]. Also, spleens of *Il23*^{KO}*Tnfaip3*$^{CD11c\text{-}KO}$ mice were enlarged in comparison to *Il23*^{KO} control mice, but they were significantly smaller than spleens of *Il23*^{WT}*Tnfaip3*$^{CD11c\text{-}KO}$ mice (**Figure 1A**). Despite the large size of the spleens in *Il23*^{KO}*Tnfaip3*$^{CD11c\text{-}KO}$mice, their cellularity was drastically reduced compared to *Il23*^{KO}*Tnfaip3*$^{CD11c\text{-}WT}$mice and to *Il23*^{WT}*Tnfaip3*$^{CD11c\text{-}KO}$mice (**Figure 1A**).

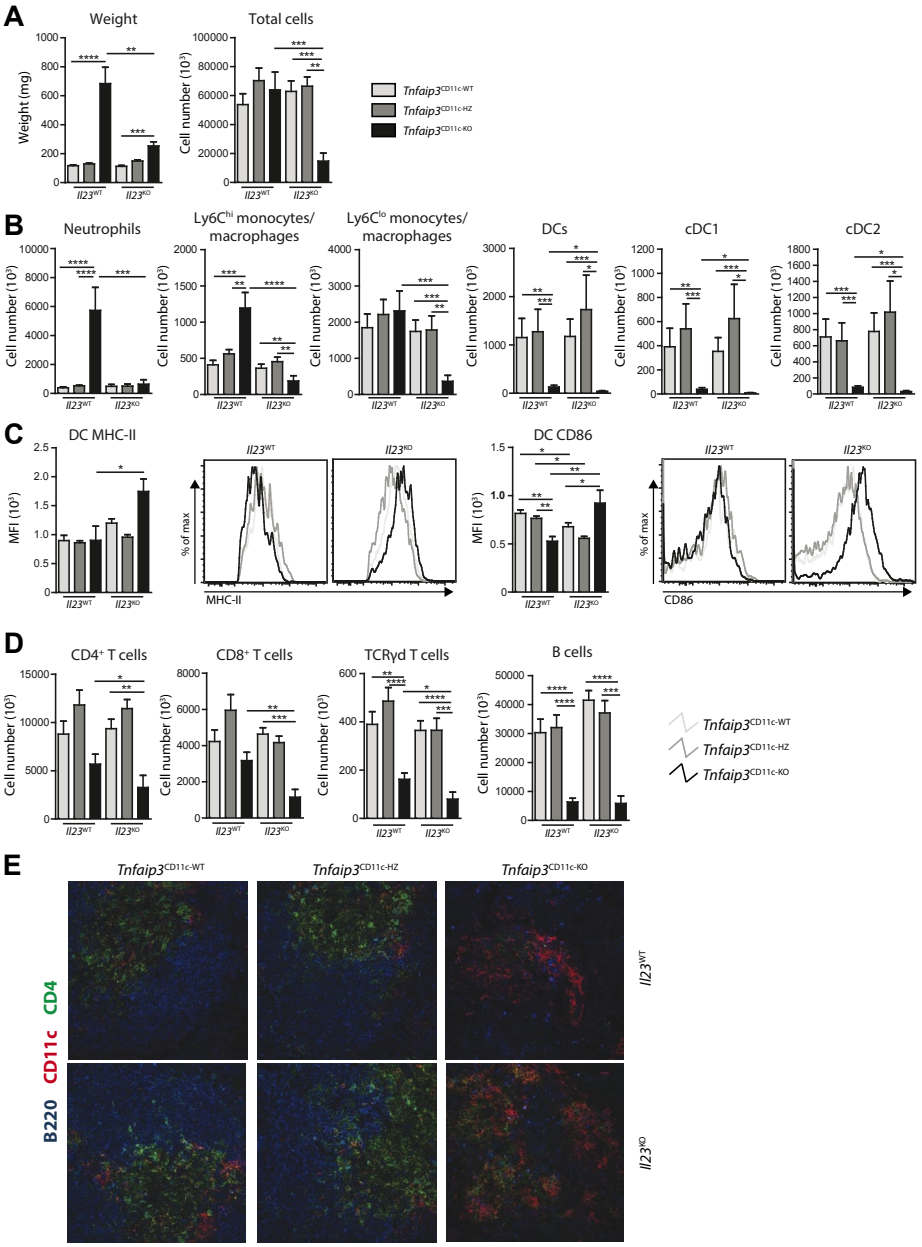

Figure 1: IL-23-deficiency strongly reduces myeloid cell populations in *Tnfaip3*$^{CD11c\text{-}KO}$ mice, but has moderate effects on lymphoid cells.

Spleens from 24-week-old naïve mice of the indicated genotypes were analyzed for myeloid and lymphoid cells. (**A**) Quantification of splenic weight and cellularity. (**B**) Enumeration of splenic neutrophils ($CD45^+CD11b^+GR1^+$), $Ly6C^{hi}$ monocytes/macrophages ($CD45^+CD11b^+GR1^-Ly6C^{hi}$), $Ly6C^{lo}$ monocytes/macrophages ($CD45^+CD11b^+GR1^-Ly6C^{lo}$), total DCs ($CD45^+CD11c^+$MHC-$II^+CD11b^-$) and cDC2s ($CD45^+CD11c^+$MHC-$II^+CD11b^+$), using flow cytometry. (**C**) Quantification surface

expression of MHC-II and CD86 on splenic DCs, using flow cytometry (*left*) and representative histogram overlays (*right*). (**D**) Quantification of splenic $CD4^+$ T cells ($CD3^+CD4^+CD8^-$), $CD8^+$ Th cells ($CD3^+CD8^+CD4^-$), TCRγδ T cells ($CD3^+TCR\gamma\delta^+$) and B cells ($B220^+CD138^-$) using flow cytometry. (**E**) Confocal imaging of spleens for CD4 (Green), B220 (Blue) and CD11c (Red). Pooled data is shown from four independent experiments (in A/B/D) and a single experiment (in C/E). Results are presented as mean values ± SEM of n = 2-19 mice per group. Kruskal-Wallis test for multiple comparisons was performed and followed by a Mann-Whitney U test. *P<0.05, **P<0.01, ***P<0.001, ****P<0.0001.

The numbers of neutrophils were significantly increased in *Il23*^{WT}*Tnfaip3*$^{CD11c\text{-}KO}$ mice, compared to WT mice, *Tnfaip3*$^{CD11c\text{-}HZ}$ mice and *Il23*^{KO}*Tnfaip3*$^{CD11c\text{-}KO}$ mice (**Figure 1B**; see for gating strategy[21]: **Supplementary Figure S1**). Whereas absolute cell counts of $Ly6C^{hi}$ monocytes/macrophage were increased in *Il23*^{WT}*Tnfaip3*$^{CD11c\text{-}KO}$ mice, compared to *Il23*^{WT} *Tnfaip3*$^{CD11c\text{-}WT}$ and *Tnfaip3*$^{CD11c\text{-}HZ}$ mice, they did not differ for the $Ly6C^{lo}$ monocyte/macrophage population (**Figure 1B**, see for gating strategy: **Supplementary Figure S1**). Both $Ly6C^{hi}$ and $Ly6c^{lo}$ monocytes were reduced in *Il23*^{KO}*Tnfaip3*$^{CD11c\text{-}KO}$ mice compared to the other mouse groups (**Figure 1B**).

The absolute numbers of total DCs, as well as the cDC1 and cDC2 subsets (see for gating strategy: **Supplementary Figure S1**), were strongly reduced in the spleens of *Il23*^{WT}*Tnfaip3*$^{CD11c\text{-}KO}$ mice and even significantly further reduced in *Il23*^{KO}*Tnfaip3*$^{CD11c\text{-}KO}$ mice, compared to their *Tnfaip3*$^{CD11c\text{-}WT}$ and *Tnfaip3*$^{CD11c\text{-}HZ}$ counterparts (**Figure 1B**). Next, we evaluated splenic DCs for the expression of the MHC class II and CD86 surface markers, which are associated with DC activation. Surface MHC-II was significantly increased in *Il23*^{KO}*Tnfaip3*$^{CD11c\text{-}KO}$ mice, compared to *Il23*^{WT}*Tnfaip3*$^{CD11c\text{-}KO}$ mice (**Figure 1C**). While CD86 expression was significantly reduced in *Il23*^{WT}*Tnfaip3*$^{CD11c\text{-}KO}$ mice, compared to *Tnfaip3*$^{CD11c\text{-}WT}$ and*Tnfaip3*$^{CD11c\text{-}HZ}$ mice, it was significantly higher in *Il23*^{KO}*Tnfaip3*$^{CD11c\text{-}KO}$ mice compared to *Il23*^{KO} mice and *Il23*^{WT}*Tnfaip3*$^{CD11c\text{-}KO}$ mice (**Figure 1C**).

In conclusion, the concomitant absence of IL-23 in *Tnfaip3*$^{CD11c\text{-}KO}$ mice resulted in significantly reduced splenic cell counts, with lower numbers of neutrophils, monocytes/macrophage and in particular DCs. The DCs in these *Il23*^{KO}*Tnfaip3*$^{CD11c\text{-}KO}$ mice had a more activated phenotype.

Lack of IL-23 has moderate effects on lymphocyte cells in the spleen.

At 24 weeks of age, the numbers of splenic $CD4^+$ T cells and $CD8^+$ T cells did not differ between *Tnfaip3*$^{CD11c\text{-}KO}$ and *Tnfaip3*$^{CD11c\text{-}WT}$ mice on the *Il23*^{WT} background (**Figure 1D**). However, they were moderately reduced in *Il23*^{KO} *Tnfaip3*$^{CD11c\text{-}KO}$ mice, compared to *Il23*^{WT}*Tnfaip3*$^{CD11c\text{-}KO}$ mice (**Figure 1D**). Both $TCR\gamma\delta^+$ T cells and B cells were reduced in *Tnfaip3*$^{CD11c\text{-}KO}$ mice, irrespective of the *Il23* genotype, when compared to the other four groups of mice (**Figure 1D**).

The very low absolute cell counts of the spleens of *Tnfaip3*$^{CD11c\text{-}KO}$*Il23*^{KO} mice, prompted us to investigated their architecture. We previously observed a disturbed splenic

architecture in *Tnfaip3*$^{CD11c\text{-}KO}$ mice in comparison to *Tnfaip3*$^{CD11c\text{-}WT}$ and *Tnfaip3*$^{CD11c\text{-}HZ}$ mice[16]. Likewise, also on the *Il23*^{KO} background the *Tnfaip3*$^{CD11c\text{-}KO}$ mice had spleens with a disturbed architecture: very few B220$^+$ cells, and a few clusters of CD11c$^+$ cells, without clearly separated B and T cell areas (**Figure 1E**). In a smaller magnification, immunohistochemical analyses revealed a drastic reduction of IgD$^+$ B cells in the spleens of both *Il23*^{WT} and *Il23*^{KO} *Tnfaip3*$^{CD11c\text{-}KO}$ mice, compared to the *Tnfaip3*$^{CD11c\text{-}WT}$ counterparts (**Supplementary Figure S2**). Large regions were devoid of IgD$^+$ B cells, most likely representing red pulp areas with myeloid cells. Nevertheless, the absence of IL-23 appeared to result in a slight rescue of IgD$^+$ B cells clusters in *Tnfaip3*$^{CD11c\text{-}KO}$ spleens. This would be consistent with the flow cytometry findings of reduced total numbers of cells, but similar numbers of B cells in the spleens of *Il23*^{KO}*Tnfaip3*$^{CD11c\text{-}KO}$ mice, compared with *Il23*^{WT} *Tnfaip3*$^{CD11c\text{-}KO}$ mice.

In conclusion, despite the substantial reduction of spleen weight and total cell count in *Il23*^{KO} *Tnfaip3*$^{CD11c\text{-}KO}$ mice compared to *Il23*^{WT} *Tnfaip3*$^{CD11c\text{-}KO}$ mice, T cell numbers were only moderately reduced and B cell numbers were comparable between the two mouse groups.

IL-23-deficiency reduces the numbers of both Th17 and non-Th17 cycling T cells in *Tnfaip3*$^{CD11c\text{-}KO}$ mice.

Because IL-23 plays a primary role in Th17-cell homeostasis and is important for the expansion of Th17 cells[10, 22], we further investigated splenic CD4$^+$ T-cell subsets.

Antigen-experienced CD44$^+$ effector and memory CD4$^+$ T cells in the spleen were highest in both *Il23*^{WT} and *Il23*^{KO} *Tnfaip3*$^{CD11c\text{-}HZ}$ mice (**Figure 2A**). This population was decreased in *Il23*^{KO}*Tnfaip3*$^{CD11c\text{-}KO}$ mice compared to *Il23*^{WT}*Tnfaip3*$^{CD11c\text{-}KO}$ mice. This was probably linked to the overall reduction of splenic CD4$^+$ T cells in *Il23*^{KO}*Tnfaip3*$^{CD11c\text{-}KO}$ mice: when we calculated the proportions of antigen-experienced CD44$^+$ effector and memory CD4$^+$ T cells as a percentage of total CD4$^+$ T cells, there was no detectable effect of the loss of IL-23 (**Supplementary Figure S3A**).

Loss of IL-23 also did not appear to affect the total numbers of RORγt$^+$ Th17 cells in the spleen of *Tnfaip3*$^{CD11c\text{-}KO}$ mice (**Figure 2B, 2C**), although their proportions within the total CD4$^+$ T cell population in the spleen were increased (**Supplementary Figure S3B**).

The numbers of cycling Ki67$^+$ CD4$^+$ T cells, non-Th17 cells and CD8$^+$ T cells in the spleen of the six groups of mice essentially reflected the total numbers of cells in these populations (**Figure 2D;** see for proportions of Ki67$^+$ cells within these populations: **Supplementary Figure S3C**). In contrast, a pattern emerged that both the absolute numbers and the proportions of Ki67$^+$ RORγt$^+$ Th17 cells were reduced in the three *Il23*^{KO} genotypes, compared with the *Il23*^{WT} counterparts (**Figure 2D**; **Supplementary Figure S3C**).

The numbers of intracellular IL-17$^+$, IFN-γ$^+$ and IL-10$^+$ splenic CD4$^+$ T cells were significantly reduced in both *Il23*^{WT} and *Il23*^{KO} *Tnfaip3*$^{CD11c\text{-}KO}$ mice, compared to their *Tnfaip3*$^{CD11c\text{-}WT}$ or *Tnfaip3*$^{CD11c\text{-}HZ}$ counterparts (**Figure 2E,2F,2G**). However, as a proportion of CD4$^+$ T cells, IL17$^+$, IFNγ$^+$ and IL-10$^+$ cells were significantly higher in *Il23*^{KO}*Tnfaip3*$^{CD11c\text{-}KO}$ mice compared to *Il23*^{KO}*Tnfaip3*$^{CD11c\text{-}WT}$ or *Il23*^{KO}*Tnfaip3*$^{CD11c\text{-}HZ}$ controls (**Supplementary Figure S3D, S3E, S3F**).

Absence of IL-23 had limited effects on the numbers of antigen-experienced CD44$^+$ effector and memory CD8$^+$ T cells in the spleen of the three mouse genotypes. Although *Il23*^{KO}*Tnfaip3*$^{CD11c\text{-}KO}$ mice had lower absolute numbers of CD44$^+$CD8$^+$ T cells than *Il23*^{WT}*Tnfaip3*$^{CD11c\text{-}KO}$ mice (**Figure 2H**), their frequencies (as proportions of CD8$^+$ T cells) were increased (**Supplementary Figure S3G**). In parallel, the absolute numbers of IFNγ$^+$ CD8$^+$ T cells tended to be lower in *Il23*^{KO}*Tnfaip3*$^{CD11c\text{-}KO}$ than in *Il23*^{WT}*Tnfaip3*$^{CD11c\text{-}KO}$ mice (**Figure 2I**), but their frequencies (as proportions of CD8$^+$ T cells) were increased (**Supplementary Figure S3H**).

In conclusion, in *Tnfaip3*$^{CD11c\text{-}KO}$ mice the lack of IL-23 did not reduce the absolute numbers or proportions of RORγ$^+$ or IL-17$^+$ Th17 cells in the spleen. Nevertheless, in these mice the absolute numbers of cycling Ki67$^+$Th17 cells, as well as the proportions of Ki67$^+$ cells within the Th17 population was reduced in the spleen in the absence of IL-23. These findings suggest that an ongoing induction of Th17 cells can compensate for the absence of IL-23-driven expansion of Th17 cells in *Il23*^{KO}*Tnfaip3*$^{CD11c\text{-}KO}$mice.

IL-23-deficiency reduces splenic plasma cells numbers and IgA serum levels in *Tnfaip3*$^{CD11c\text{-}KO}$ mice.

Since Th17 cells are known to mediate B cell differentiation and Ig heavy chain class switch recombination[7], we assessed the effects of *Il23* gene deletion on germinal center (GC) B cells and plasma cells in the spleen at the age of 24 weeks. GC B-cell numbers were reduced in *Tnfaip3*$^{CD11c\text{-}KO}$ mice, irrespective of the presence of IL-23 (**Figure 3A**). However, as a proportion of B cells, splenic GC B cells were enhanced in *Tnfaip3*$^{CD11c\text{-}KO}$ mice and also in *Il23*^{KO}*Tnfaip3*$^{CD11c\text{-}HZ}$ mice, compared to *Tnfaip3*$^{CD11c\text{-}WT}$ mice and *Il23*^{KO} mice respectively (**Supplementary Figure 4A**). Splenic plasma cell numbers were elevated in *Il23*^{WT}*Tnfaip3*$^{CD11c\text{-}HZ}$ mice in comparison to *Il23*^{WT}*Tnfaip3*$^{CD11c\text{-}WT}$ and *Il23*^{WT}*Tnfaip3*$^{CD11c\text{-}KO}$ mice (**Figure 3A**). Importantly, whereas the effect of the absence of IL-23 on *Tnfaip3*$^{CD11c\text{-}WT}$ and *Tnfaip3*$^{CD11c\text{-}HZ}$ mice was limited, plasma cells were very low in *Il23*^{KO}*Tnfaip3*$^{CD11c\text{-}KO}$ mice (**Figure 3A).** This pattern was similar for IgM$^+$, IgG1$^+$ and IgA$^+$ plasma cell counts (**Figure 3A**). When we analyzed the Ig heavy chain class distribution in the plasma cells, we noticed that proportions of IgG1$^+$ plasma cells were increased in *Tnfaip3*$^{CD11c\text{-}KO}$ mice, in particular in *Il23*^{KO}*Tnfaip3*$^{CD11c\text{-}KO}$ mice, compared to *Tnfaip3*$^{CD11c\text{-}WT}$ mice on an *Il23*^{WT} or *Il23*^{KO} background (**Supplementary Figure 4B,** see also pie-chart).

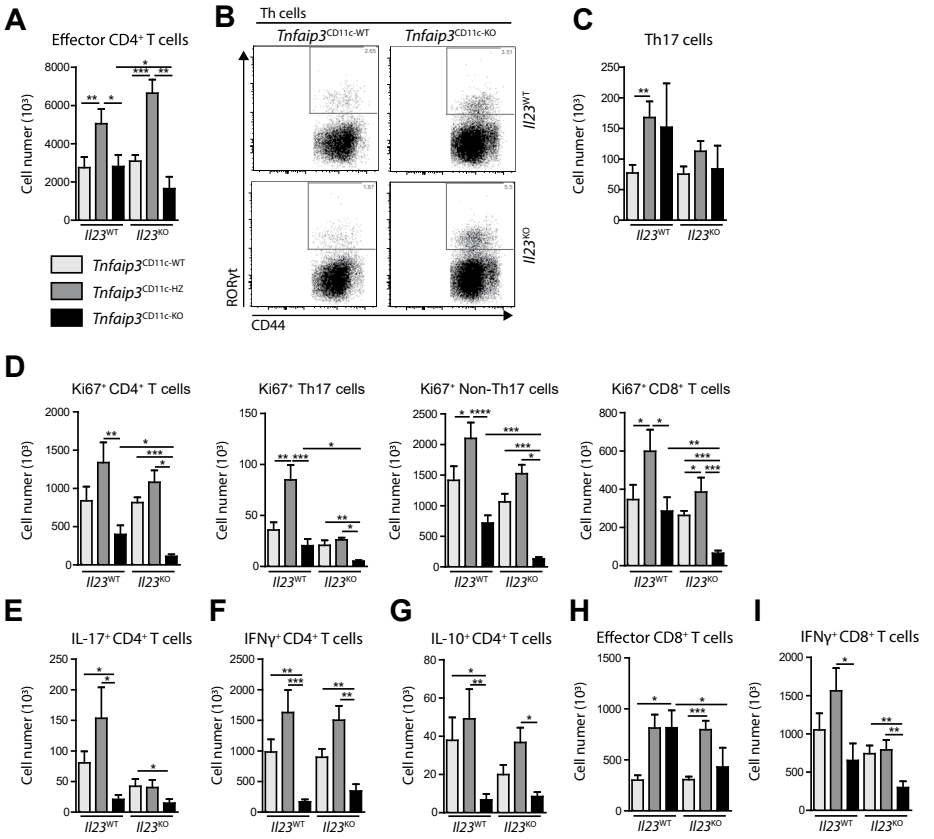

Figure 2: IL-23-deficiency reduces the numbers of both Th17 and non-Th17 cycling T cells in *Tnfaip3*$^{CD11c\text{-}KO}$ mice.

Spleens from 24-week-old naïve mice of the indicated genotypes were analyzed for T cell populations. (**A**) Quantification of splenic antigen-experienced effector CD4$^+$ T cells (CD3$^+$CD4$^+$CD44$^+$) using flow cytometry. (**B-C**) Flow cytometry profiles of gated CD4$^+$ T cells for surface CD44 and intracellular RORγt$^+$ (**B**) and enumeration of splenic Th17 cells (CD3$^+$CD4$^+$RORγt$^+$)(**C**) using flow cytometry. (**D**) Quantification of Ki67$^+$ proliferating CD4$^+$ T cells (CD3$^+$CD4$^+$Ki67$^+$), Th17 cells (CD3$^+$CD4$^+$Roryt$^+$Ki67$^+$), Non-Th17 cells (CD3$^+$CD4$^+$Roryt$^-$Ki67$^+$) and CD8$^+$ T cells (CD3$^+$CD8$^+$Ki67$^+$) (**E-I**) Quantification of IL-17$^+$ CD4$^+$ T cells (CD3$^+$CD4$^+$IL-17$^+$) (**E**), IFNγ$^+$ CD4$^+$ T cells (CD3$^+$CD4$^+$IFNγ$^+$) (**F**), IL-10$^+$ CD4$^+$ T cells (CD3$^+$CD4$^+$IL-10$^+$) (**G**) antigen experienced effector CD8$^+$ T cells (CD3$^+$CD8$^+$CD44$^+$) (**H**) and IFNγ$^+$ CD8$^+$ T cells (CD3$^+$CD8$^+$IFNγ$^+$) (**I**), using flow cytometry. Pooled data are shown from four independent experiments, except for panels D, E and G, which were from two independent experiments. Results are presented as mean values ± SEM of *n* = 3-19 mice per group. Kruskal-Wallis test for multiple comparisons was performed and followed by a Mann-Whitney U test. *P<0.05, **P<0.01, ***P<0.001, ****P<0.0001.

The remaining fraction of splenic plasma cells, expressing IgG2b, IgG2c and IgG3 appeared to be increased in the absence of IL-23.

The total numbers of B220$^+$ B-lineage cells in the bone marrow (BM) of *Il23*^{WT}*Tnfaip3*$^{CD11c\text{-}KO}$ mice were significantly decreased (**Figure 3B**), pointing to a developmental

B cell defect (described in greater detail in chapter 5 of this thesis) and thus providing an explanation for the reduced numbers of B cells present in the spleen of these mice. Also, the absolute numbers of total plasma cells were highest in *Il23*^{WT} *Tnfaip3*$^{CD11c\text{-}HZ}$ mice, but reduced in *Il23*^{WT} and *Il23*^{KO} *Tnfaip3*$^{CD11c\text{-}KO}$ mice compared to the other mouse groups (**Figure 3B**). All three *Tnfaip3* genotypes had lower numbers of IgM$^+$ plasma cells on the *Il23*^{KO} than on the *Il23*^{WT} background. IgM$^+$ plasma cells were virtually absent in *Il23*^{KO} *Tnfaip3*$^{CD11c\text{-}KO}$ mice (**Figure 3B**). In contrast, the complete absence of Tnfaip3/A20 or IL-23 did not significantly affect the numbers of BM IgG1$^+$ or IgA$^+$ plasma cells. An IL-23-dependent rise was seen for BM IgG1$^+$ and IgA$^+$ BM plasma cells in *Tnfaip3*$^{CD11c\text{-}HZ}$ mice compared to the control mice (**Figure 3B**).

Altogether, regarding the Ig heavy chain class distribution in BM plasma cells, we observed a reduction of the proportions of IgM$^+$ plasma cells in *Il23*^{WT}*Tnfaip3*$^{CD11c\text{-}KO}$ mice and a virtual absence of IgM$^+$ plasma cells in *Il23*^{KO}*Tnfaip3*$^{CD11c\text{-}KO}$ mice (**Supplementary Figure 4C**, see also pie-chart). Concomitantly, the proportions of BM IgG1$^+$ and IgA$^+$ plasma cells were increased in *Tnfaip3*$^{CD11c\text{-}KO}$ mice compared to *Tnfaip3*$^{CD11c\text{-}WT}$ mice and *Tnfaip3*$^{CD11c\text{-}HZ}$ mice, irrespective of the presence of IL-23 (**Supplementary Figure 4C**, see also pie-chart).

Next, we assessed serum Ig levels and observed a differential effect of the absence of Tnfaip3/A20 on individual subclasses: IgM and Ig2b were unaffected, IgG1 and IgA were increased and IgG2c and IgG3 were decreased (**Figure 3C**). In *Il23*^{WT}*Tnfaip3*$^{CD11c\text{-}HZ}$ mice, we found that only IgA levels were increased. For most subclasses this pattern was largely unaffected by the absence of IL-23, except that levels of IgA were lower in all three *Il23*^{KO} *Tnfaip3* genotypes compared to their *Il23*^{WT} equivalents (**Figure 3C**). Thus, in *Il23*^{KO}*Tnfaip3*$^{CD11c\text{-}KO}$ mice the levels of IgA in serum were in the normal range, similar to *Il23*^{WT}*Tnfaip3*$^{CD11c\text{-}WT}$ mice.

In summary, the absence of IL-23 resulted in strong reduction of IgM$^+$, IgG1$^+$ and IgA$^+$ splenic plasma cells specifically in the group of *Tnfaip3*$^{CD11c\text{-}KO}$ mice. By contrast, in the BM the absence of IL-23 reduced the numbers of IgM$^+$ plasma cells in all three *Tnfaip3* genotypes, but did not significantly affect IgG1$^+$ and IgA$^+$ plasma cell counts in *Tnfaip3*$^{CD11c\text{-}KO}$ mice. Serum IgG1 and IgA were the primary isotypes increased in *Tnfaip3*$^{CD11c\text{-}KO}$ mice, but additional loss of IL-23 in these mice only reduced serum IgA levels, leaving IgG1 levels unaffected.

IL-23-deficiency does not affect autoreactive IgG1 levels or kidney glomerulonephritis in *Tnfaip3*$^{CD11c\text{-}KO}$ mice.

Since aged *Tnfaip3*$^{CD11c\text{-}KO}$ mice expressed autoantibodies *in vivo*[16], we analyzed the presence of autoreactive anti-dsDNA and anti-cardiolipin IgG1 in serum of 24-week-old mice. Anti-dsDNA and anti-cardiolipin IgG1 was higher in *Tnfaip3*$^{CD11c\text{-}KO}$ mice than *Tnfaip3*$^{CD11c\text{-}HZ}$ or *Tnfaip3*$^{CD11c\text{-}KO}$ mice, regardless of IL-23-deficiency, although this

did not reach significance (**Figure 4A, 4B**). Since autoreactive immunoglobulins may cause tissue damage in glomeruli, we assessed histology of the kidney glomeruli in the six groups of mice. We previously reported that aged *Tnfaip3*$^{CD11c\text{-}KO}$ mice developed membranoproliferative glomerulonephritis with increased glomerular cellularity and thickening of the basement membranes[16]. Using PAS-D staining we confirmed that ~80% of the *Il23*^{WT}*Tnfaip3*$^{CD11c\text{-}KO}$ mice had thicker glomerular basement membranes, compared to 0% and ~25% in *Il23*^{WT}*Tnfaip3*$^{CD11c\text{-}WT}$ and *Il23*^{WT}*Tnfaip3*$^{CD11c\text{-}HZ}$ mice respectively (**Figure 4C**). Lack of IL-23 lead to similar basement membrane thickening in 100% of *Il23*^{KO} *Tnfaip3*$^{CD11c\text{-}KO}$ mice compared to 0% and ~40% in *Il23*^{KO}*Tnfaip3*$^{CD11c\text{-}WT}$ and *Il23*^{KO}*Tnfaip3*$^{CD11c\text{-}HZ}$ mice respectively (**Figure 4C**).

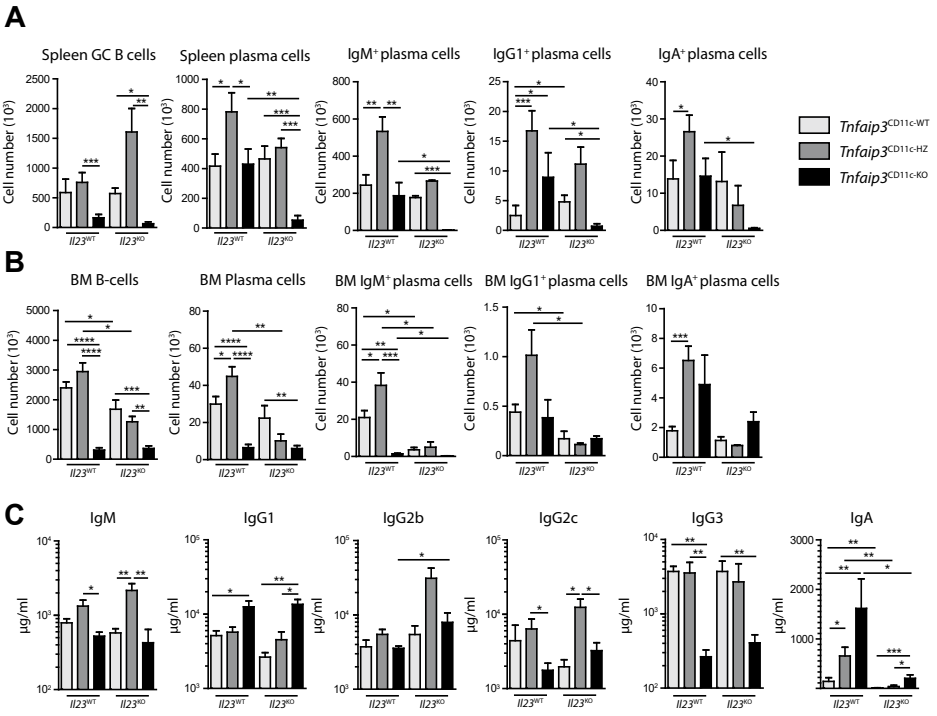

Figure 3: IL-23-deficiency reduces splenic plasma cells numbers and IgA serum levels in *Tnfaip3*$^{CD11c\text{-}KO}$ mice.

Spleens and bone marrow (BM) from 24-week-old naïve mice of the indicated genotypes were analyzed for B-cell populations. (**A-B**) Quantification of GC B-cells (B220^{+}CD138^{-}IgD^{-}CD95^{+}), plasma cells (B220^{-}CD138^{+}), IgM^{+} plasma cells (B220^{-}CD138^{+}IgM^{+}), IgG1^{+} plasma cells (B220^{-}CD138^{+}IgG1^{+}) and IgA^{+} plasma cells B-cells (B220^{-}CD138^{+}IgA^{+}) in spleens (**A**) and BM (**B**) (Total B-lineage cells in BM gated as B220^{+}CD138^{-}) using flow cytometry. (**C**) Serum concentrations of IgM, IgG1, IgG2b, IgG2c, IgG3 and IgA, determined by ELISA. Pooled data are shown from three independent experiments (panels A and B). Serum Ig levels are from two (IgM, IgG2b, IgG2c, IgG3) or four (IgG1, IgA) independent experiments. Results are presented as mean values ± SEM of *n* = 5-15 mice per group. Kruskal-Wallis test for multiple comparisons was performed and followed by a Mann-Whitney U test. *P<0.05, **P<0.01, ***P<0.001, ****P<0.0001.

Thus, lack of IL-23 did not abrogate the formation of IgG1 autoantibodies nor thickening of the glomerular basement membrane in *Tnfaip3*$^{CD11c\text{-}KO}$ mice.

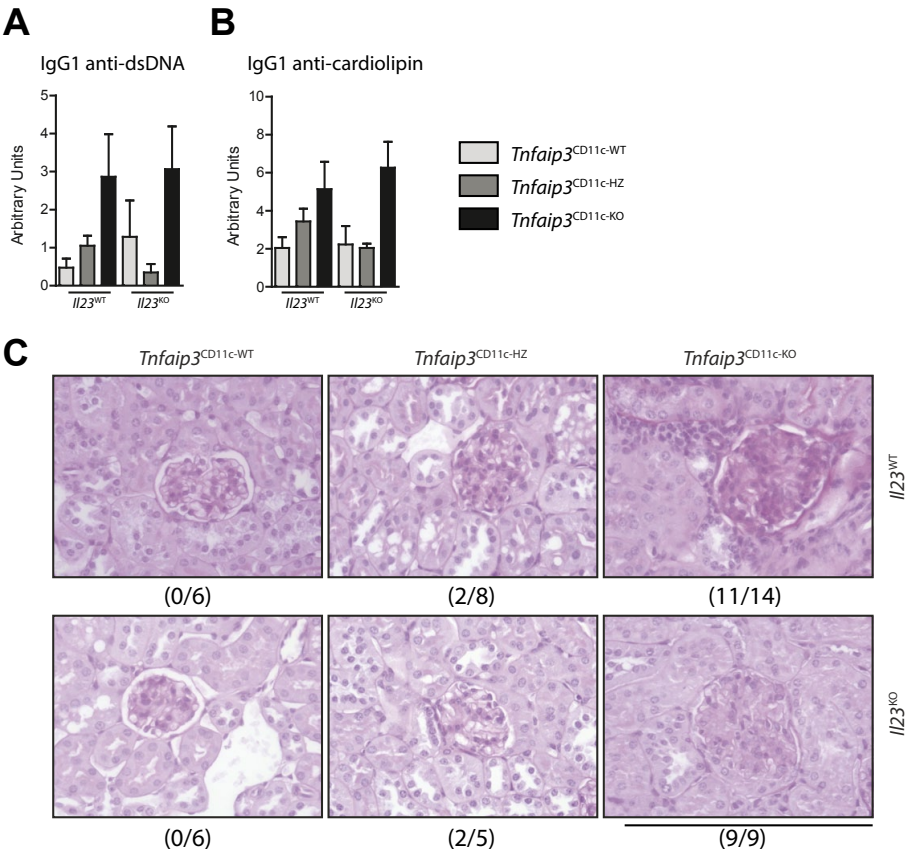

Figure 4: IL-23-deficiency does not affect autoreactive IgG1 levels or kidney glomerulonephritis in *Tnfaip3*$^{CD11c\text{-}KO}$ mice.

Serum of naïve 24-week-old mice of the indicated genotypes was analyzed for autoreactive IgG1 towards dsDNA (**A**) and cardiolipin (**B**) using ELISA. (**C**) PAS-D staining on paraffin-embedded kidneys. Scale bars represent 200µm. Representative histology images are shown from three independent experiments. Results are presented as mean values ± SEM of *n* = 2-10 mice per group.

DISCUSSION

Since the start of the millennium, the discovery of IL-23 and the primary acting cytokine IL-17 has redefined the understanding of autoimmune disorders[22]. In several autoimmune disorders such as psoriasis, inflammatory bowel disease (IBD) or SLE, common subunit p40 blockade of IL-12 and IL-23 or selective blockade of IL-23 has shown

promising clinical results[15, 23]. Also, in lupus mouse models the role of IL-23/IL-17 is of importance[24]. We studied our *Tnfaip3*$^{CD11c\text{-}KO}$ lupus mouse model, in which Tnfaip3/A20, a negative regulator for NF-κB, is specifically deleted in DCs, leading to hyperactivated DCs[16]. As a result, activity of T and B cells is dysregulated and mice express autoantibodies and develop lupus nephritis. BM-derived DCs from *Tnfaip3*$^{CD11c\text{-}KO}$ mice produced high IL-23 and induced Th17 cell differentiation *in vitro*[16]. In this report, we addressed the question whether loss of IL-23 *in vivo* would restore Th17 cell homeostasis and thereby alleviate the lupus phenotype. We found, however, that *in vivo* Th17 cell differentiation was not enhanced in 24-week-old *Tnfaip3*$^{CD11c\text{-}KO}$ mice, compared to *Tnfaip3*$^{CD11c\text{-}WT}$ mice. Moreover, loss of IL-23 expression did not significantly affect the numbers of Th17 cells in the spleen, serum levels of IgG1 or anti-dsDNA IgG1 or kidney glomerulonephritis. Taken together, these findings indicate that the autoimmune pathology in *Tnfaip3*$^{CD11c\text{-}KO}$ mice is independent of the IL-23/IL-17 axis.

While *Tnfaip3*$^{CD11c\text{-}KO}$ mice had enlarged spleens with various proliferating myeloid cells[16], these were significantly reduced in the absence of IL-23. This was possibly due to survival signals to myeloid cells provided by IL-23, as shown during *C. albicans* infection[25]. Neutrophils were the myeloid cells that expanded most in *Il23*^{WT}*Tnfaip3*$^{CD11c\text{-}KO}$ mice. Although IL-23 deficiency may be associated with defects in granulopoiesis[26, 27], no differences were seen between *Il23*^{WT}and *Il23*^{KO} mice of the *Tnfaip3*$^{CD11c\text{-}WT}$ or *Tnfaip3*$^{CD11c\text{-}HZ}$ genotype.

All conventional DC subsets, including the cDC2 subset known to primarily produce IL-23[28] were reduced in number, both in *Il23*^{WT} and *Il23*^{KO} *Tnfaip3*$^{CD11c\text{-}KO}$ mice. Surprisingly, splenic DC activation status, as measured by surface MHC-II and CD86 expression was higher in *Il23*^{KO} than *Il23*^{WT} *Tnfaip3*$^{CD11c\text{-}KO}$ mice. *In vitro,* Tnfaip3/A20-deficient BM-derived DCs showed no differences for CD40, CD86 or MHC-II expression between IL-23^{WT} and IL-23^{KO} mice, indicating that IL-23 had no effect on their activation status *in vitro*. An autocrine effect of IL-23 on DCs has been suggested, influencing IL-12 production and improving antigen presentation in a skin reactivity test[29, 30]. Furthermore, human *in vitro* studies show that IL-23 promotes T cell proliferation, without affecting DC maturation[31]. In a naïve state only ~4% of CD11c^{+} DCs express IL-23R[32]. This did not differ across the six mouse groups in our study (T.D., unpublished. data), suggesting that the absence of this autocrine IL-23 effect is not a likely explanation for enhanced activation of DCs in *Il23*^{KO}*Tnfaip3*$^{CD11c\text{-}KO}$ mice. In contrast to previous findings[16], we saw a reduction of splenic DCs at the age of 24 weeks in *Il23*^{WT} *Tnfaip3*$^{CD11c\text{-}KO}$ mice, and even more so in *Il23*^{KO}*Tnfaip3*$^{CD11c\text{-}KO}$ mice. It may be argued that a higher activation status of this minor population of DCs is not likely to contribute to the systemic phenotype in *Il23*^{KO}*Tnfaip3*$^{CD11c\text{-}KO}$ mice. However, despite having such low DC counts, both *Il23*^{WT} and *Il23*^{KO}*Tnfaip3*$^{CD11c\text{-}KO}$ mice still developed the lupus-like phenotype. This suggests that secondary activated cells that were in proximity to the DCs, such as T-cells or monocytes/macrophages contribute to the

phenotype, e.g. by elevated cytokine production such as the previously demonstrated IL-6 and TNF-α[16].

In contrast to previously reported *in vitro* studies[16], *Tnfaip3*$^{CD11c\text{-}KO}$ mice did not have increased RORγt^{+} Th17 cells or IL-17^{+} CD4^{+} T cells *in vivo,* compared to *Tnfaip3*$^{CD11c\text{-}WT}$ mice. It remains however unclear whether this originates from differences between *in vivo* and *in vitro* findings, or from differences between mouse facilities or microbiome. The latter would be supported by our analyses of the B cell compartment in the spleens of 24-week-old *Tnfaip3*$^{CD11c\text{-}KO}$ mice, showing reduced numbers of GC B cells and similar numbers of plasma cells compared to WT control mice, whereas Kool *et al.* reported that both cell populations were increased (although not significantly) in 25-week-old *Tnfaip3*$^{CD11c\text{-}KO}$ mice[16]. In this context, it is of note that another strain of C57Bl/6 mice with a DC-specific deficiency of Tnfaip3/A20, also based on CD11c-Cre-mediated gene targeting developed a phenotype characterized by IBD-associated arthritis[33]. This phenotype is quite different from the SLE-like phenotype in our *Tnfaip3*$^{CD11c\text{-}KO}$ mice[16], which would support an important role of microbiome or other environmental factors on the *in vivo* immunological and pathological effects of Tnfaip3/A20 deletion.

We were surprised to see that whereas antigen-experienced effector/memory CD4^{+} T-cells were reduced in the spleens of *Il23*^{KO}*Tnfaip3*$^{CD11c\text{-}KO}$ mice, this was not observed for RORγt^{+} Th17 cells or IL-17^{+} CD4^{+} T cells. Rather, the proportions of RORγt^{+} Th17 cells and IL-17^{+} CD4^{+} T cells appeared to rise in *Il23*^{KO}*Tnfaip3*$^{CD11c\text{-}KO}$ mice compared to *Il23*^{WT}*Tnfaip3*$^{CD11c\text{-}KO}$ mice. Two roles of IL-23 have been proposed, namely induction of T cell expansion and induction of T cell pathogenicity. Whereas initially IL-23 was regarded as an inducing factor for Th17 cells[34], later studies show that primarily TGF-β and IL-6 are responsible for the induction and IL-23 is more important for survival and expansion of Th17 cells[12]. T cell proliferation was overall reduced in *Il23*^{KO} mice, however, as a proportion of CD4^{+} T cells, only the Th17 cell population - and not non-Th17 cells - showed a reduction in proliferation due to absence of IL-23. The limited effects of IL-23 on the size of the splenic Th17 population, together with a reduction of Ki67^{+} proliferating Th17 cells, suggest an ongoing *de novo* induction of Th17 cells, or an increased migration of resting Th17 cells into the spleen. Both of these mechanisms may compensate for the absence of IL-23-driven expansion of Th17 cells in *Il23*^{KO}*Tnfaip3*$^{CD11c\text{-}KO}$mice.

Another concept would be that IL-23 unlocks the full pathogenic potential of autoreactive T-cells, while only the TGF-β/IL-6 combination induces more suppressive IL-10^{+} T-cells[13]. Indeed, in our data a significant increase of the proportions – but not absolute numbers - of splenic IL-10^{+} T-cells was seen in *Il23*^{KO}*Tnfaip3*$^{CD11c\text{-}KO}$ mice, compared to *Il23*^{WT}*Tnfaip3*$^{CD11c\text{-}KO}$ mice, suggesting that relatively more immunosuppressive CD4^{+} T cells were present in the absence of IL-23. In our hands cytokine and transcription factor expression could unfortunately not reliably be combined to analyze on the single-cell level whether RORγt^{+} Th17 cells had altered IL-10 production. Regardless of these

suppressive IL-10^{+} Th-cells, however, autoantibody production or tissue inflammation assessed by basement membrane thickening in kidney glomeruli was unaltered in *Tnfaip3*$^{CD11c\text{-}KO}$ mice in absence of IL-23. Further experiments are necessary to determine whether other Th17-associated cytokines, such as IL-22 and GM-CSF, which is normally induced by IL-23[35], are changed in *Il23*^{WT} and *Il23*^{KO}*Tnfaip3*$^{CD11c\text{-}KO}$ mice.

The numbers of splenic IL-17^{+} or IFNγ^{+} Th cells was not different between *Il23*^{WT} and *Il23*^{KO}*Tnfaip3*$^{CD11c\text{-}KO}$ mice. As a proportion, however, substantial increases in IFNγ^{+} Th cells were seen. This is not likely caused by IL-23-deficiency alone, because IL-23 has only a marginal effect on IFNγ expression[36]. Although IL-23 does not induce Th17 commitment, it helps to maintain a Th17 phenotype[37], which might explain why in its absence higher levels of Th1 cytokines are produced when DCs have an activated phenotype. Nevertheless, although it has been shown that plasticity of Th17 cells towards IFNγ^{+} Th1 cells is dependent on IL-23[38], we did not find evidence for such a role of IL-23 in our *Tnfaip3*$^{CD11c\text{-}KO}$ mice: IL-17^{+}IFNγ^{+} Th cells were not decreased in *Il23*^{KO} *Tnfaip3*$^{CD11c\text{-}KO}$ mice (T.D., unpublished data). Taken together, our findings suggests that the proportions of IFNγ^{+} CD4^{+} Th-cells in *Il23*^{KO} *Tnfaip3*$^{CD11c\text{-}KO}$mice may rise due to (i) *de novo* induction of Th1 cells over Th17 cells, possibly supported by IL-12 from *Tnfaip3*$^{CD11c\text{-}KO}$ DCs[17] or to (ii) migration of IFNγ^{+} CD4^{+} Th-cells into the spleen or migration of IFNγ^{-} CD4^{+} cells out of the spleen.

Th17 cells influence B-cell activation and Ig production by plasma cells into isotypes IgG1, IgG2a/c and IgG2b[7]. Since Th17 cells were not reduced in *Il23*^{KO} *Tnfaip3*$^{CD11c\text{-}KO}$ mice compared to *Il23*^{WT}*Tnfaip3*$^{CD11c\text{-}KO}$ mice, it was expected that also serum Ig levels were essentially unaffected. This was indeed the case, except that IgA was substantially reduced. Given the low numbers of IgA^{+} plasma cells in the spleens of *Tnfaip3*$^{CD11c\text{-}KO}$ *Il23*^{KO} mice, while the bone marrow plasma cells were unaffected, it might be possible that a major fraction of serum IgA in *Tnfaip3*$^{CD11c\text{-}KO}$ mice was produced in the spleen. However, IgA could also be derived from the intestine[39], but we did not observe intestinal autoimmune inflammation in *Il23*^{WT} or *Il23*^{KO}*Tnfaip3*$^{CD11c\text{-}KO}$ mice (T.D., unpublished data), despite a previous report of gut inflammation in another published *Tnfaip3*$^{CD11c\text{-}KO}$ mouse model[33]. Yet, lack of IL-23 did not appear to affect the autoimmune phenotype in that a similar basement membrane thickening was found in the kidney glomeruli of *Il23*^{WT} and *Il23*^{KO}*Tnfaip3*$^{CD11c\text{-}KO}$ mice. Given the differential effects of the absence of Tnfaip3/A20 or IL-23-deficiency on the individual subclasses, additional experiments are required to evaluate the autoreactivity of the individual Ig subclasses in the serum of *Il23*^{WT} and *Il23*^{KO}*Tnfaip3*$^{CD11c\text{-}KO}$ mice. Likewise, it will be informative to investigate the presence and nature of immune complex depositions in the glomeruli in *Il23*^{WT} and *Il23*^{KO}*Tnfaip3*$^{CD11c\text{-}KO}$ mice.

In conclusion, the absence of IL-23 resulted in a substantial reduction of granulocytes and monocytes/macrophage in the spleens of *Tnfaip3*$^{CD11c\text{-}KO}$ mice. Although

splenic DCs from *Il23*^{KO}*Tnfaip3*$^{CD11c\text{-}KO}$ had a more activated phenotype than DCs from *Il23*^{WT}*Tnfaip3*$^{CD11c\text{-}KO}$ mice, their numbers remained very low. Deletion of the *Tnfaip3* gene in DCs did not enhance Th17 cell differentiation *in vivo* and further loss of IL-23 did not affect the numbers of splenic Th17 cells. Despite a severe reduction of plasma cells in the spleen, the serum of *Il23*^{KO}*Tnfaip3*$^{CD11c\text{-}KO}$ mice contained autoreactive IgG1. Glomerular membrane thickening seen in *Tnfaip3*$^{CD11c\text{-}KO}$ mice was also unaffected by IL-23-deficiency. From these findings we conclude that the autoimmune pathology in *Tnfaip3*$^{CD11c\text{-}KO}$ mice is independent of the IL-23/IL-17 axis.

Acknowledgements

We would like to thank Odilia Corneth and the Erasmus MC Animal Facility (EDC) staff for their assistance during the project. This project was supported by The Dutch Arthritis Association (12-2-410) and the European Framework program 7 (FP7-MC-CIG grant 304221).

Conflict of interest

The authors declare no conflict of interest.

REFERENCES

1. Crispin JC, Liossis SN, Kis-Toth K, Lieberman LA, Kyttaris VC, Juang YT *et al.* Pathogenesis of human systemic lupus erythematosus: recent advances. *Trends in molecular medicine* 2010; 16(2): 47-57.
2. Nashi E, Wang Y, Diamond B. The role of B cells in lupus pathogenesis. *The international journal of biochemistry & cell biology* 2010; 42(4): 543-550.
3. Flores-Mendoza G, Sanson SP, Rodriguez-Castro S, Crispin JC, Rosetti F. Mechanisms of Tissue Injury in Lupus Nephritis. *Trends in molecular medicine* 2018; 24(4): 364-378.
4. Wong CK, Lit LC, Tam LS, Li EK, Wong PT, Lam CW. Hyperproduction of IL-23 and IL-17 in patients with systemic lupus erythematosus: implications for Th17-mediated inflammation in auto-immunity. *Clinical immunology (Orlando, Fla)* 2008; 127(3): 385-393.
5. Xing Q, Wang B, Su H, Cui J, Li J. Elevated Th17 cells are accompanied by FoxP3+ Treg cells decrease in patients with lupus nephritis. *Rheumatology international* 2012; 32(4): 949-958.
6. Hsu HC, Yang P, Wang J, Wu Q, Myers R, Chen J *et al.* Interleukin 17-producing T helper cells and interleukin 17 orchestrate autoreactive germinal center development in autoimmune BXD2 mice. *Nature immunology* 2008; 9(2): 166-175.
7. Mitsdoerffer M, Lee Y, Jager A, Kim HJ, Korn T, Kolls JK *et al.* Proinflammatory T helper type 17 cells are effective B-cell helpers. *Proceedings of the National Academy of Sciences of the United States of America* 2010; 107(32): 14292-14297.
8. Amarilyo G, Lourenco EV, Shi FD, La Cava A. IL-17 promotes murine lupus. *Journal of immunology (Baltimore, Md : 1950)* 2014; 193(2): 540-543.
9. McGeachy MJ, Chen Y, Tato CM, Laurence A, Joyce-Shaikh B, Blumenschein WM *et al.* The interleukin 23 receptor is essential for the terminal differentiation of interleukin 17-producing effector T helper cells in vivo. *Nature immunology* 2009; 10(3): 314-324.
10. Oppmann B, Lesley R, Blom B, Timans JC, Xu Y, Hunte B *et al.* Novel p19 protein engages IL-12p40 to form a cytokine, IL-23, with biological activities similar as well as distinct from IL-12. *Immunity* 2000; 13(5): 715-725.
11. Ghoreschi K, Laurence A, Yang XP, Tato CM, McGeachy MJ, Konkel JE *et al.* Generation of pathogenic T(H)17 cells in the absence of TGF-beta signalling. *Nature* 2010; 467(7318): 967-971.
12. Veldhoen M, Hocking RJ, Atkins CJ, Locksley RM, Stockinger B. TGFbeta in the context of an inflammatory cytokine milieu supports de novo differentiation of IL-17-producing T cells. *Immunity* 2006; 24(2): 179-189.
13. McGeachy MJ, Bak-Jensen KS, Chen Y, Tato CM, Blumenschein W, McClanahan T *et al.* TGF-beta and IL-6 drive the production of IL-17 and IL-10 by T cells and restrain T(H)-17 cell-mediated pathology. *Nature immunology* 2007; 8(12): 1390-1397.
14. Larosa M, Zen M, Gatto M, Jesus D, Zanatta E, Iaccarino L *et al.* IL-12 and IL-23/Th17 axis in systemic lupus erythematosus. *Experimental biology and medicine (Maywood, NJ)* 2019; 244(1): 42-51.
15. van Vollenhoven RF, Hahn BH, Tsokos GC, Wagner CL, Lipsky P, Touma Z *et al.* Efficacy and safety of ustekinumab, an IL-12 and IL-23 inhibitor, in patients with active systemic lupus erythematosus: results of a multicentre, double-blind, phase 2, randomised, controlled study. *Lancet (London, England)* 2018; 392(10155): 1330-1339.
16. Kool M, van Loo G, Waelput W, De Prijck S, Muskens F, Sze M *et al.* The ubiquitin-editing protein A20 prevents dendritic cell activation, recognition of apoptotic cells,

and systemic autoimmunity. *Immunity* 2011; 35(1): 82-96.

17. Vroman H, Bergen IM, van Hulst JAC, van Nimwegen M, van Uden D, Schuijs MJ *et al.* TNF-alpha-induced protein 3 levels in lung dendritic cells instruct TH2 or TH17 cell differentiation in eosinophilic or neutrophilic asthma. *The Journal of allergy and clinical immunology* 2018; 141(5): 1620-1633. e1612.
18. Ghilardi N, Kljavin N, Chen Q, Lucas S, Gurney AL, De Sauvage FJ. Compromised humoral and delayed-type hypersensitivity responses in IL-23-deficient mice. *Journal of immunology (Baltimore, Md : 1950)* 2004; 172(5): 2827-2833.
19. Vroman H, Bergen IM, Li BW, van Hulst JA, Lukkes M, van Uden D *et al.* Development of eosinophilic inflammation is independent of B-T cell interaction in a chronic house dust mite-driven asthma model. *Clinical and experimental allergy : journal of the British Society for Allergy and Clinical Immunology* 2017; 47(4): 551-564.
20. Das T, Bergen IM, Koudstaal T, van Hulst JAC, van Loo G, Boonstra A *et al.* DNGR1-mediated deletion of A20/Tnfaip3 in dendritic cells alters T and B-cell homeostasis and promotes autoimmune liver pathology. *Journal of autoimmunity* 2019; 102: 167-178.
21. Cossarizza A, Chang HD, Radbruch A, Acs A, Adam D, Adam-Klages S *et al.* Guidelines for the use of flow cytometry and cell sorting in immunological studies (second edition). *European journal of immunology* 2019; 49(10): 1457-1973.
22. Gaffen SL, Jain R, Garg AV, Cua DJ. The IL-23-IL-17 immune axis: from mechanisms to therapeutic testing. *Nature reviews Immunology* 2014; 14(9): 585-600.
23. Kashani A, Schwartz DA. The Expanding Role of Anti-IL-12 and/or Anti-IL-23 Antibodies in the Treatment of Inflammatory Bowel Disease. *Gastroenterology & hepatology* 2019; 15(5): 255-265.
24. Kyttaris VC, Zhang Z, Kuchroo VK, Oukka M, Tsokos GC. Cutting edge: IL-23 receptor deficiency prevents the development of lupus nephritis in C57BL/6-lpr/lpr mice. *Journal of immunology (Baltimore, Md : 1950)* 2010; 184(9): 4605-4609.
25. Nur S, Sparber F, Lemberg C, Guiducci E, Schweizer TA, Zwicky P *et al.* IL-23 supports host defense against systemic Candida albicans infection by ensuring myeloid cell survival. *PLoS pathogens* 2019; 15(12): e1008115.
26. Smith E, Zarbock A, Stark MA, Burcin TL, Bruce AC, Foley P *et al.* IL-23 is required for neutrophil homeostasis in normal and neutrophilic mice. *Journal of immunology (Baltimore, Md : 1950)* 2007; 179(12): 8274-8279.
27. Stark MA, Huo Y, Burcin TL, Morris MA, Olson TS, Ley K. Phagocytosis of apoptotic neutrophils regulates granulopoiesis via IL-23 and IL-17. *Immunity* 2005; 22(3): 285-294.
28. Satpathy AT, Briseno CG, Lee JS, Ng D, Manieri NA, Kc W *et al.* Notch2-dependent classical dendritic cells orchestrate intestinal immunity to attaching-and-effacing bacterial pathogens. *Nature immunology* 2013; 14(9): 937-948.
29. Belladonna ML, Renauld JC, Bianchi R, Vacca C, Fallarino F, Orabona C *et al.* IL-23 and IL-12 have overlapping, but distinct, effects on murine dendritic cells. *Journal of immunology (Baltimore, Md : 1950)* 2002; 168(11): 5448-5454.
30. Li Y, Yu X, Ma Y, Hua S. IL-23 and dendritic cells: What are the roles of their mutual attachment in immune response and immunotherapy? *Cytokine* 2019; 120: 78-84.
31. Vaknin-Dembinsky A, Balashov K, Weiner HL. IL-23 is increased in dendritic cells in multiple sclerosis and down-regulation of IL-23 by antisense oligos increases dendritic cell IL-10 production. *Journal of immunology (Baltimore, Md : 1950)* 2006; 176(12): 7768-7774.

32. Awasthi A, Riol-Blanco L, Jager A, Korn T, Pot C, Galileos G *et al.* Cutting edge: IL-23 receptor gfp reporter mice reveal distinct populations of IL-17-producing cells. *Journal of immunology (Baltimore, Md : 1950)* 2009; 182(10): 5904-5908.
33. Hammer GE, Turer EE, Taylor KE, Fang CJ, Advincula R, Oshima S *et al.* Expression of A20 by dendritic cells preserves immune homeostasis and prevents colitis and spondyloarthritis. *Nature immunology* 2011; 12(12): 1184-1193.
34. Harrington LE, Hatton RD, Mangan PR, Turner H, Murphy TL, Murphy KM *et al.* Interleukin 17-producing CD4+ effector T cells develop via a lineage distinct from the T helper type 1 and 2 lineages. *Nature immunology* 2005; 6(11): 1123-1132.
35. El-Behi M, Ciric B, Dai H, Yan Y, Cullimore M, Safavi F *et al.* The encephalitogenicity of T(H)17 cells is dependent on IL-1- and IL-23-induced production of the cytokine GM-CSF. *Nature immunology* 2011; 12(6): 568-575.
36. Chackerian AA, Chen SJ, Brodie SJ, Mattson JD, McClanahan TK, Kastelein RA *et al.* Neutralization or absence of the interleukin-23 pathway does not compromise immunity to mycobacterial infection. *Infection and immunity* 2006; 74(11): 6092-6099.
37. Stritesky GL, Yeh N, Kaplan MH. IL-23 promotes maintenance but not commitment to the Th17 lineage. *Journal of immunology (Baltimore, Md : 1950)* 2008; 181(9): 5948-5955.
38. Hirota K, Duarte JH, Veldhoen M, Hornsby E, Li Y, Cua DJ *et al.* Fate mapping of IL-17-producing T cells in inflammatory responses. *Nature immunology* 2011; 12(3): 255-263.
39. Gutzeit C, Magri G, Cerutti A. Intestinal IgA production and its role in host-microbe interaction. *Immunological reviews* 2014; 260(1): 76-85.

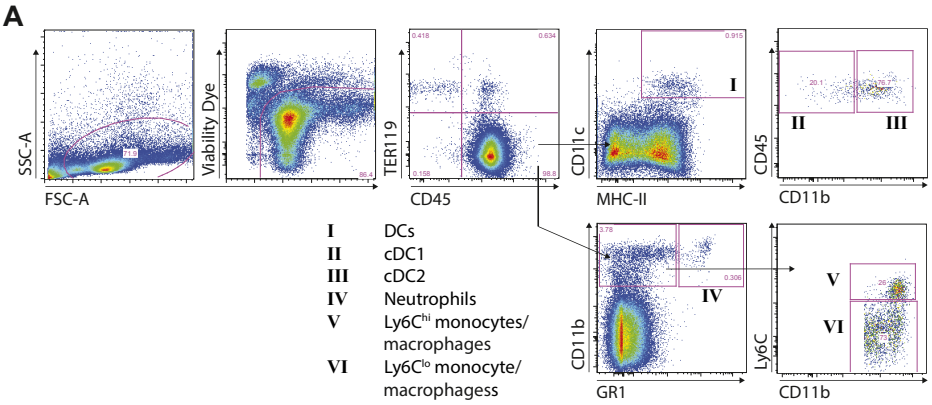

Supplementary Figure 1: Gating strategy for the indicated myeloid cell fractions in the spleen of naïve 24-week-old mice, using flow cytometry.

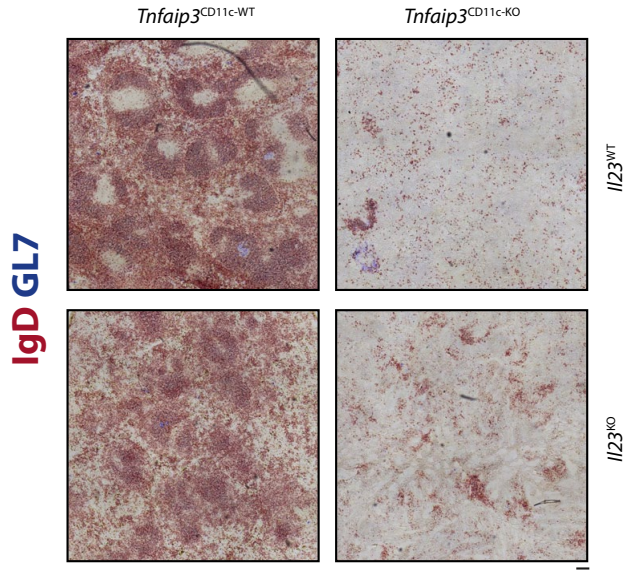

Supplementary Figure 2: IL-23-deficiency has no major effects on the splenic architecture in *Tnfaip3*$^{CD11c\text{-}KO}$ mice.

Spleens from naïve 24-week-old mice from the indicated genotypes were analyzed by immunohistochemistry for IgD (Red) and GL7 (Blue). Scale bars represent 200μm.

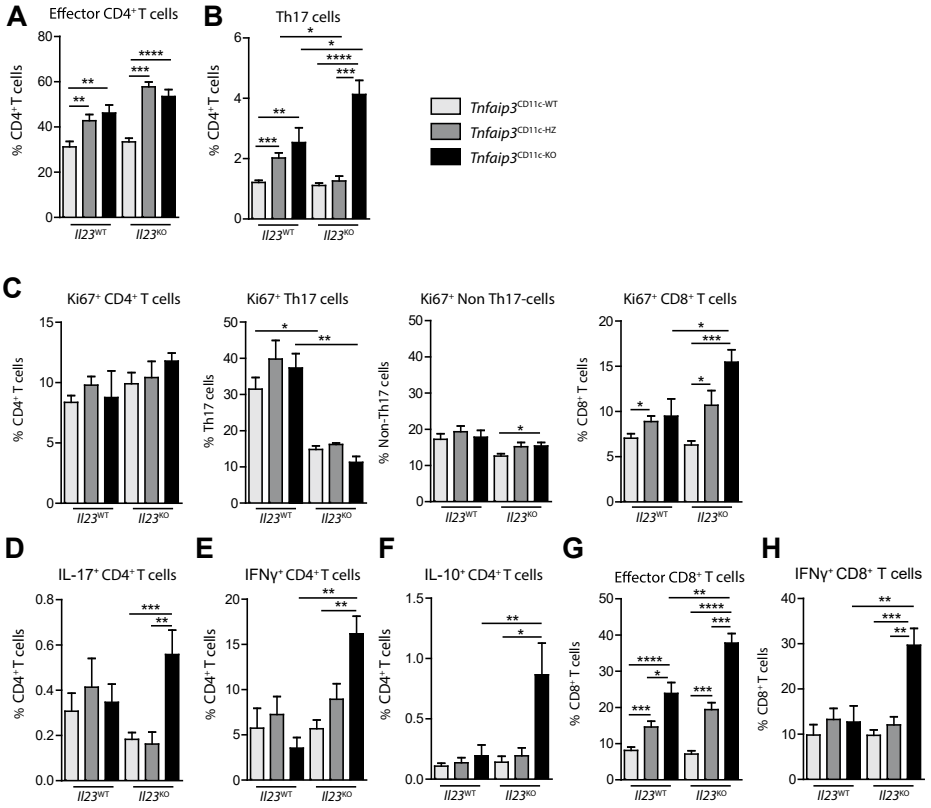

Supplementary Figure 3: Effects of IL-23-deficiency on the proportions of T cell subsets, T cell proliferation and cytokine production.

Spleens from naïve 24-week-old mice from the indicated genotypes were analyzed for T cell populations. (**A-B**) Quantification of proportions splenic effector CD4+ T-cells ($CD3^+CD4^+CD44^+$)(A) and $ROR\gamma t^+$ Th17 cells ($CD3^+CD4^+ROR\gamma t^+$) (**B**) using flow cytometry. (**C**) Quantification of proportions $Ki67^+$ proliferating $CD4^+$ T cells ($CD3^+CD4^+Ki67^+$), Th17 cells ($CD3^+CD4^+Ror\gamma t^+Ki67^+$), Non-Th17 cells ($CD3^+CD4^+Ror\gamma t^-$ $Ki67^+$) and $CD8^+$ T cells ($CD3^+CD8^+$ $Ki67^+$) (**D-H**) Proportion $IL\text{-}17^+$ $CD4^+$ T cells ($CD3^+CD4^+IL\text{-}17^+$) (**D**) $IFN\gamma^+$ $CD4^+$ T cells ($CD3^+CD4^+IFN\gamma^+$) (**E**) and $IL\text{-}10^+$ $CD4^+$ T cells ($CD3^+CD4^+IL\text{-}10^+$)(**F**) and effector $CD8^+$ T-cells ($CD3^+CD8^+CD44^+$) (**G**) and $IFN\gamma^+$ $CD8^+$ T-cells ($CD3^+CD8^+IFN\gamma^+$) (**H**) using flow cytometry. Pooled data are shown from four independent experiments, except for panels C,D and F, which are from two independent experiments. Results are presented as mean values ± SEM of n = 3-19 mice per group. Kruskal-Wallis test for multiple comparisons was performed, followed by a Mann-Whitney U test. *P<0.05, **P<0.01, ***P<0.001, ****P<0.0001.

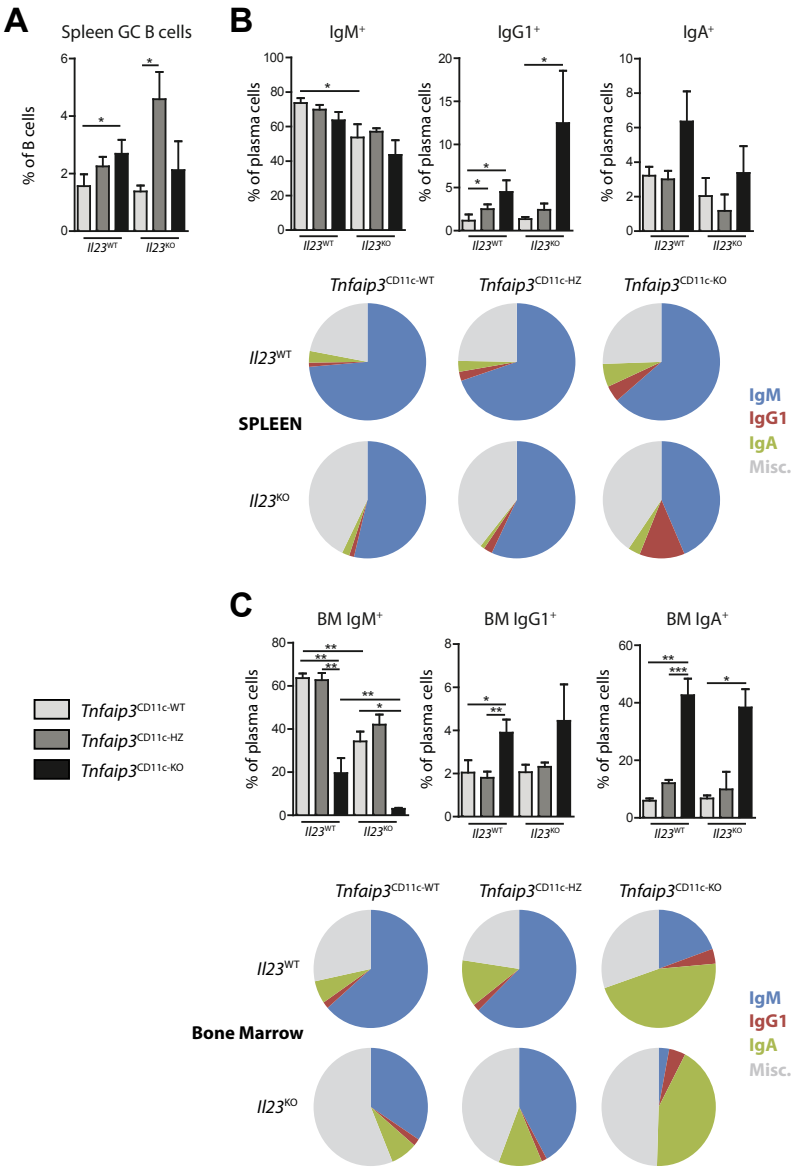

Supplementary Figure 4: Splenic and BM proportions of IgA$^+$ and IgG1$^+$ plasma cells are elevated regardless of IL-23 in *Tnfaip3*$^{CD11c\text{-}KO}$ mice.

Naïve 24-week-old *Tnfaip3*^{CD11c}*Il23* mice spleens and BM were analyzed for B cell and plasma cell proportions. (**A**) Quantification of proportion splenic GC B cells (B220$^+$IgD$^-$CD95$^+$) using flow cytometry. (**B-C**) Enumeration of the proportion IgM$^+$ plasma cells (B220$^-$CD138$^+$IgM$^+$), IgG1$^+$ plasma cells (B220$^-$CD138$^+$IgG1$^+$) and IgA$^+$ plasma cells (B220$^-$CD138$^+$IgA$^+$) in spleen (**B**) and BM (**C**) using flow cytometry. Pie charts have been included of these proportions. Pooled data is shown from three independent experiments, except panels (**B/C**) which are from one experiment. Results are presented as mean values ± SEM of n = 2-15 mice per group. Kruskal-Wallis test for multiple comparisons was used, followed by Mann-Whitney U test. *P<0.05, **P<0.01, ***P<0.001.

Supplementary Table 1: Antibodies used for flow cytometry

Antibody	Conjugate	Clone	Company
B220	AF700	RA3-6B2	eBioscience
CD11b	PercP-Cy5.5	M1/70	BD
CD11c	BV786	HL3	BD
CD138	BV605	281-2	BD
CD19	APC-Cy7	1D3	BD
CD3e	PE-CF594	145-2C11	BD
CD4	BV711	RM4-5	BD
CD44	Percp-Cy5.5	IM7	eBioscience
CD44	APC-cy7	IM7	BD
CD45	PE TxR	I3/2.3	Abcam
CD62L	APC-Cy7	MEL-14	BD
CD8a	PE-Cy7	53-6.7	eBioscience
CD86	PE-Cy7	GL1	BD
Gr-1	PE-Cy7	D7	eBioscience
IFN-y	ef450	XMG1.2	eBioscience
IgD	APC	11-26c	eBioscience
IgG1	Biotin	A85-1	BD
IgG2a/b	Biotin	R2-40	BD
IgG3	Biotin	R40-82	BD
IgM	PE-Cy7	II/41	eBioscience
IL-10	Percp-EF710	JES5-16E3	eBioscience
IL17A	AF700	TC11-18A10.1	BD
Ki67	eFluor 660	SolA15	eBioscience
MHC II	AF700	I-Ad/I-Ed	eBioscience
RORyt	PE	Q31-378	BD